Thermal properties of magnons in yttrium iron garnet at elevated magnetic fields

S. M. Rezende* and J. C. López Ortiz
Departamento de Física, Universidade Federal de Pernambuco, 50670-901 Recife PE, Brazil
(Received 25 November 2014; revised manuscript received 4 March 2015; published 19 March 2015)

The ferrimagnetic insulator yttrium iron garnet (YIG) has become an important material in the emergent field of spin caloritronics. Despite this and the fact that this material has been studied for over half a century, the thermal properties of magnons in YIG have not been sufficiently characterized, mainly because at not very low temperatures, they are overwhelmed by the contribution of phonons. Experimental attempts to characterize the magnon specific heat and thermal conductivity in YIG make use of large magnetic fields to freeze the magnon contributions and isolate those of phonons relative to their behavior at zero field. Here we present calculations of the magnon thermal properties in YIG under elevated magnetic fields using spin-wave theory. We show that at a temperature of 10 K, a field of at least 300 kOe is necessary to decrease the magnon contributions to 10% of their zero-field values. With the results of the calculations, we reinterpret recent measurements of the magnon thermal properties in YIG at temperatures up to 20 K and a field of 70 kOe, and suggest a procedure to determine their values at room temperature with the use of a field of 300 kOe.

DOI: 10.1103/PhysRevB.91.104416 PACS number(s): 75.30.Ds, 75.40.−s, 75.76.+j

I. INTRODUCTION

At present, insulator-based spintronics relies almost entirely on the unique properties of the ferrimagnetic insulator yttrium iron garnet [$Y_3Fe_5O_{12}$ (YIG)]. In recent years YIG has gained increased attention for revealing striking features of the spin Hall [1–5] and spin Seebeck effects [6–16], but for several decades it has been the prototype material for the study of the basic physics of a variety of spin-wave phenomena [17–26]. The recent upsurge in the interest in YIG has resulted in the intensification of research on new methods to grow crystalline thin films and in the study of basic material properties with more sophisticated equipment than those used in the early investigations [27]. One of the current challenges is to quantify the thermal properties of magnons in YIG at room temperature since they are essential to clarify the origin of the spin Seebeck effect in structures containing this material. A serious difficulty is that at temperatures above 5 K the thermal properties of YIG are dominated by the behavior of phonons, so that the contributions from magnons become difficult to measure.

Early experimental attempts to characterize the magnon specific heat and thermal conductivity in YIG at temperatures (T) below 5 K employed the application of magnetic fields up to 40 kOe to open a gap in the magnon dispersion to freeze the magnon contributions and isolate those of phonons relative to their behavior at zero field [28,29]. But even at low T it was recognized early on that theory and data for the magnon thermal conductivity were discrepant [29]. Recently, Boona and Heremans [30] used a larger magnetic field (70 kOe) in an attempt to freeze the magnon contributions, and claim to have measured the absolute values of the magnon specific heat and thermal conductivity in YIG at temperatures up to 20 K. This connects with broader field-induced thermal conductivity phenomena, which have received significant interest recently in the context of quantum antiferromagnets, where gaps can be induced or closed by the application of a magnetic field [31].

In this paper we present calculations of the changes in the thermal properties of magnons in YIG produced by the application of high magnetic fields based on spin-wave theory. The recent experimental data are reinterpreted and shown to not represent the full quantities, but only changes in the magnon contributions with the application of the field. We show that at a temperature of 10 K, a field of at least 300 kOe is necessary to decrease the magnon contributions to 10% of their zero-field values. Based on the good agreement between theory and data, we suggest a procedure to determine the magnon thermal properties accurately at room temperature with the use of a field of 300 kOe.

II. SPIN WAVES IN YIG AT HIGH FIELDS

The thermal properties of magnons depend crucially on the wave-vector-dependent magnon frequency, velocity, and lifetime. The first two are given directly by the magnon dispersion relations, which were calculated for YIG long ago [32] and later measured over the whole Brillouin zone by inelastic neutron scattering [33]. The data in zero-field, which are in fair agreement with calculations, show an acoustic branch with frequency that rises from nearly zero at the zone center to a value at the zone boundary that varies from 6 to 9.5 THz depending on the wave vector direction. These values correspond to energies of approximately 287 and 454 K. Since the lowest optical branch lies above the zone-boundary value, the calculation of the thermal properties in the presence of an applied field H at temperatures up to 100 K can be safely done considering only the acoustic branch, with the magnon dispersion relation given by [34]

$$\omega_k = \gamma H + \omega_{ZB}\left(1 - \cos\frac{\pi k}{2k_m}\right), \tag{1}$$

where $\gamma = g\mu_B/\hbar$ is the gyromagnetic ratio, g is the spectroscopic splitting factor, μ_B the Bohr magneton, $\hbar$ the reduced Plank constant, ω_{ZB} the zone-boundary frequency, and k_m is the value of the maximum wave number. At low wave numbers the dispersion relation in Eq. (1) can be approximated by the

*Corresponding author: rezende@df.ufpe.br

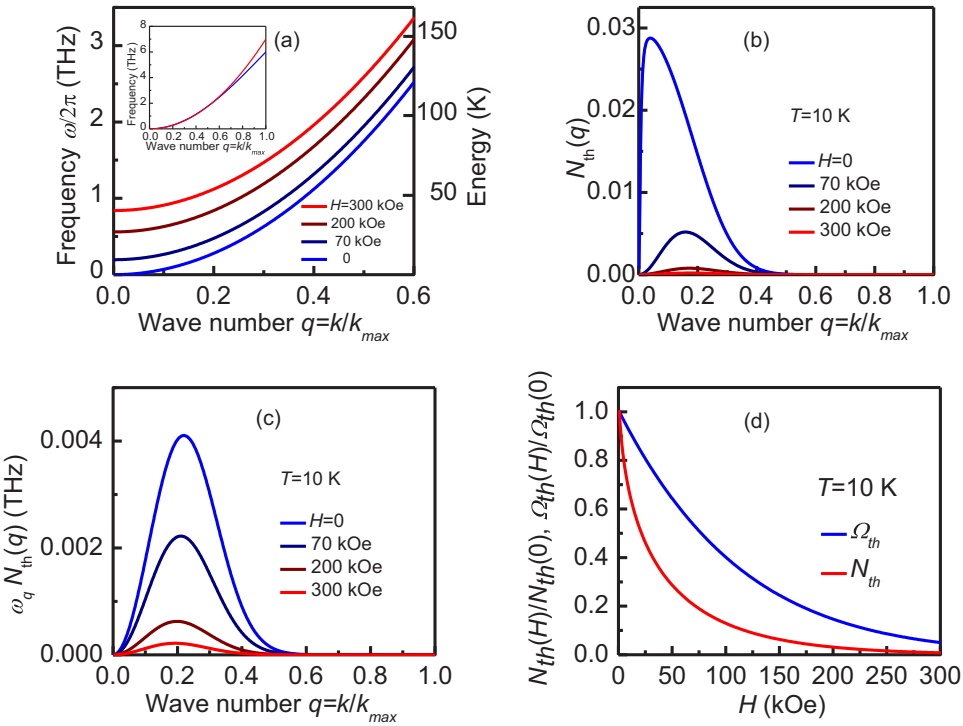

FIG. 1. (Color online) (a) Spin-wave dispersions in YIG calculated with the quadratic form in Eq. (2) for several values of the applied magnetic field H. The inset shows a comparison of the quadratic dispersion with the one in Eq. (1) over the whole Brillouin zone for $H = 0$. (b) Dependence on the reduced wave number q of the number of thermal magnons at $T = 10$ K, weighted by the density of states $N_{\rm th}(q) = \bar{n}_q q^2$ for several values of the magnetic field. (c) Variation with q of the weighted magnon frequency $\omega_q N_{\rm th}(q) = \omega_q \bar{n}_q q^2$ for several values of H. (d) Field dependence of the integrated magnon thermal number and weighted frequency at $T = 10$ K.

quadratic form

$$\omega_k = \gamma H + \gamma D k^2, \tag{2}$$

where $D = \pi^2 \omega_{\rm ZB}/(8\gamma k_m^2)$ is the exchange parameter [17,18]. Assuming spherical energy surfaces, the value of k_m that preserves the number of modes within the Brillouin zone is determined by $4\pi k_m^3/3 = (2\pi/a)^3$, where a is the lattice parameter, which gives $k_m \approx 2.45/a$. However, at low temperatures this criterion is not important because the modes with high k do not contribute to the thermal properties. One could also consider the wave number at the zone boundary in the [111] direction is $2.5\sqrt{3}/a$ [32]. In YIG, $a = 1.23 \times 10^{-7}$ cm, so k_m can be considered an adjustable parameter in the range $1.99 \times 10^7 < k_m < 3.52 \times 10^7$ cm^{-1}. Figure 1(a) shows the dispersion relations of magnons in YIG for several values of the applied field calculated with Eq. (2) using $\gamma = 2.8$ GHz/kOe and $D = 4.0 \times 10^{-9}$ Oe cm^2, the value of the exchange parameter for which the theory fits the data for the specific heat, as discussed later, which is similar to the ones quoted in the literature [17]. The inset in Fig. 1(a) shows the comparison of the quadratic dispersion with the one in Eq. (1) for zero field, calculated over the whole Brillouin zone using $\omega_{\rm ZB}/2\pi = 6.0$ THz and $k_m = 2.54 \times 10^7$ cm^{-1}. Clearly, the quadratic dispersion represents very well the actual dispersion up to a wave number $q = k/k_m = 0.6$.

As shown in Fig. 1(a), the application of a magnetic field creates in the magnon dispersion a frequency gap at $k = 0$ of 28 GHz/10 kOe, corresponding to an energy of 1.34 K/10 kOe. The increased frequency reduces the number of thermal magnons at a temperature T, given by the Bose-Einstein distribution $\bar{n}_q = 1/[\exp(\hbar\omega_q/k_B T) - 1]$. Thus, as argued in Refs. [28–30], by applying a sufficiently large field at some T, the magnon contribution to the thermal properties can be drastically reduced so that they become determined by phonons only. In this way, the changes in the thermal properties relative to the zero-field values would represent the magnetic parts. While this is true, the values of the quenching fields used in Refs. [28–30] are largely underestimated. As shown in Fig. 1(a), the gap created by a field of 70 kOe is only 9.38 K. This is more clearly demonstrated in Fig. 1(b), showing the dependence on the reduced wave number q of the number of thermal magnons at $T = 10$ K, weighted by the density of states $N_{\rm th}(q) = \bar{n}_q q^2$ for several values of the magnetic field. As expected, the weighted thermal number decreases rapidly with increasing field. However, the quantity of interest in the specific heat is the product of the thermal number with the magnon frequency, $\omega_q N_{\rm th}(q) = \omega_q \bar{n}_q q^2$. As shown in Fig. 1(c), the reduction of this quantity with field is much less pronounced. This is so because at $q \approx 0.2$, where the number peaks, the exchange contribution to the frequency is as large as the gap. This conclusion is further illustrated in Fig. 1(d), showing the variation with field of the total number of thermal magnons $N_{\rm th} = \int dq\, \bar{n}_q q^2$ and the integrated weighted frequency $\Omega_{\rm th} = \int dq\, \omega_q \bar{n}_q q^2$, relative to their values at zero field. While at $H = 70$ kOe the former is reduced to 20% of its zero-field value, the latter is reduced only to about 53%.

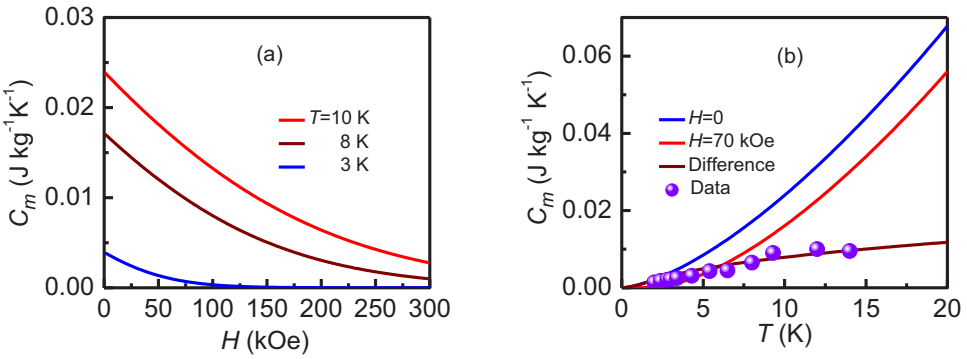

FIG. 2. (Color online) (a) Variation with magnetic field of the specific heat calculated with Eq. (3) for several temperature values. (b) Temperature dependence of the specific heat calculated with zero field and with $H = 70$ kOe. The difference is compared with the data of Ref. [30] represented by the symbols.

III. MAGNON SPECIFIC HEAT AND THERMAL CONDUCTIVITY AT ELEVATED FIELDS

The specific heat, or heat capacity per unit volume, of a magnon system in a volume V is given by $C_m = V^{-1}(\partial/\partial T)\sum_k \bar{n}_k \hbar\omega_k$, where the sum is carried out over the first Brillouin zone [18,35]. For $T < 50$ K the contribution of thermal magnons with wave number above $q = 0.5$ is very small, so one can use the quadratic dispersion in Eq. (2) and assume spherical energy surfaces. Introducing the normalized energy $x = \hbar\omega_k/k_B T$ and replacing the sum over the wave number by an integral in the usual way, one can express k in terms of x, so that the magnon specific heat becomes

$$C_m = \frac{k_B^{5/2} T^{3/2}}{4\pi^2(\gamma D\hbar)^{3/2}} \int_{x_0}^{x_m} dx \frac{e^x (x - x_0) x^2}{(e^x - 1)^2}, \qquad (3)$$

where x_m is the normalized energy with wave number k_m and $x_0 = \hbar\gamma H/k_B T$ represents the effect of the gap introduced by the magnetic field. At low temperatures the number of thermal magnons with wave number k_m is negligible so that the integral in Eq. (3) can have the upper limit set to infinity. For zero field, $x_0 = 0$, and the integral can be solved analytically to give the known result [35] $C_m = [15\varsigma(5/2)/4(4\pi\gamma D\hbar)^{3/2}]k_B^{5/2}T^{3/2}$, where $\varsigma(5/2) \approx 1.34$ is a Riemann zeta function. For nonzero field the integral has to be calculated numerically. Figure 2(a) shows the variation with field of the heat capacity per unit mass for YIG, obtained with Eq. (3) divided by the mass density ($\rho = 5.2$ for YIG). As expected, the result is very sensitive to the temperature. For $T = 3$ K the specific heat falls rapidly with increasing field, reaching about 15% of its zero-field value at $H = 70$ kOe. However, for $T = 10$ K, at $H = 70$ kOe the specific heat is as large as 2/3 of its zero-field value. In order to decrease C_m to 10% of its zero-field value, the field needed at $T = 10$ K is quite large, $H = 300$ kOe. This result indicates that the recent experimental data of Ref. [30] deserve a different interpretation. In the measurements of the thermal properties of YIG reported in Ref. [30] it was assumed that with the application of a field $H = 70$ kOe the contributions of magnons were suppressed. Thus, by measuring the specific heat as a function of temperature with $H = 0$ and 70 kOe, the difference was entirely attributed to magnons. As shown in Fig. 2(a), this is not correct. Figure 2(b) shows the calculated T dependence of the specific heat for $H = 0$ and 70 kOe, as well as their difference compared to the experimental data. The only two material parameters used in Eq. (3) are $\gamma = 2.8$ GHz/kOe, which is a well-established value for YIG [17], and $D = 4.0 \times 10^{-9}$ Oe cm^2, which was adjusted to fit the data and is similar to values quoted in the literature [17,22,26]. Thus, what the experimental data of Ref. [30] represent is the change in the magnon specific heat with applied field, not the total magnon contribution.

Similarly to the specific heat, we will show that the data in Ref. [30] for the magnon thermal conductivity K_m represent the change with magnetic field, not the full contribution. In the case of K_m the behavior becomes more interesting because of the role of the magnon relaxation rate η_k. For the calculation of K_m one considers that the flow of magnons due to a temperature gradient ∇T carries a heat-current density $\vec{J}_Q = V^{-1}\sum_k \delta n_k \hbar\omega_k \vec{v}_k$, where $\delta n_k = n_k - \bar{n}_k$ is the magnon number in excess of equilibrium and $\vec{v}_k$ is the k-magnon group velocity. Using the Boltzmann approach one can write a first-order expression for the excess magnon number in the steady state and in the relaxation approximation, $\delta n_k = -\tau_k \vec{v}_k \cdot \nabla \bar{n}_k$, where $\tau_k = 1/\eta_k$ is the k-magnon relaxation time. Assuming spherical magnon energy surfaces and considering for low T the quadratic dispersion in Eq. (2), one obtains a heat-current density in the form $\vec{J}_Q = -K_m \nabla T$, where K_m is the magnon thermal conductivity given by

$$K_m = \frac{k_B (k_B T)^{5/2}}{3\pi^2(\gamma D)^{1/2}\hbar^{5/2}} \int_{x_0}^{x_m} \frac{e^x x^2 (x - x_0)^{3/2}}{\eta_k (e^x - 1)^2} dx. \qquad (4)$$

If one considers that the relaxation rate η_k is independent of the wave number and temperature, at zero field the integral with the upper limit $x_m \to \infty$ can be solved analytically to give the temperature dependence $K_m \propto T^{5/2}$, first predicted by Yellon and Berger [36]. For nonzero field the $T^{5/2}$ still holds, but the prefactor decreases with field since $x_0 \propto H$. Figure 3(a) shows the temperature dependence of the magnon thermal conductivity in YIG calculated with Eq. (4) using $D = 4 \times 10^{-9}$ Oe cm^2 and a relaxation rate $\eta_k = 10^9$ s^{-1}, for two field values, $H = 0$ and 70 kOe. Of course, since in both cases the thermal conductivity is proportional to $T^{5/2}$, the difference between them increases continuously with temperature with the same power law. As we show next, the peak in the T dependence of the difference in the thermal conductivity measured in YIG with and without the field

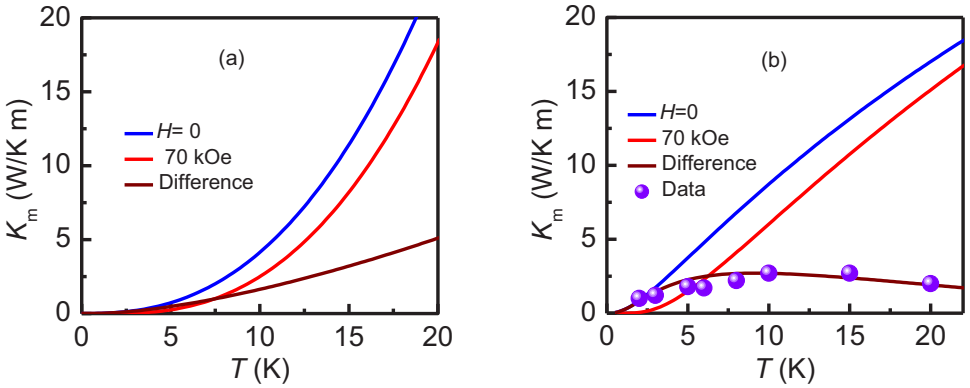

FIG. 3. (Color online) Temperature dependence of the magnon thermal conductivity calculated with Eq. (4) with $H = 0$ and 70 kOe and their difference. In (a) the magnon relaxation rate is assumed to be independent of temperature. In (b) the calculation was done with the relaxation rate in Eq. (5). The symbols in (b) represent the data of Ref. [30].

observed in Ref. [30] is due to the fact that the relaxation rate varies with wave number and temperature.

The importance of the k and T dependences of the magnon relaxation rate for the magnon thermal conductivity was first pointed out in Ref. [34]. A difficulty here is that the spin-wave damping has been measured experimentally only for very small wave numbers using microwave techniques [17,37], while the magnons that contribute most to the thermal conductivity are in the middle of the Brillouin zone, as shown in Fig. 1(c). Thus, one has to resort to calculated relaxation rates, which are at best good estimates in the absence of data to determine some adjustable parameters. We have calculated the integral in Eq. (4) the using the following expression for the magnon relaxation rate,

$$\eta_k = \eta_0\Big[1.0 + c_{H3}7.5\times 10^2 q\left(\frac{T}{300}\right) + c_{H4}10^3 \times(7.6q^2 - 4.9q^3)\left(\frac{T}{300}\right)^2\Big], \quad (5)$$

where $\eta_0 = 5\times 10^7\ \mathrm{s}^{-1}$ is the relaxation rate at $k = 0$ and $T = 0$ due to impurities and other imperfections, while the second and third terms arise, respectively, from 3- and 4-magnon scattering processes. Equation (5) with $c_{H3} = c_{H4} = 1.0$ is the relaxation rate of Ref. [34] for $H = 0$. These factors were introduced here to account for the reduction in the damping with the application of a field, as discussed later. At temperatures $T < 5$ K the relaxation is dominated by the first term, so that the thermal conductivity increases continuously with T, as observed experimentally [28,29,38]. At higher T, the relaxation rate in Eq. (5) increases with T, initially with the linear term and then with the quadratic one. As a result, the calculated magnon thermal conductivity in YIG exhibits the initial $T^{5/2}$ behavior, and then it peaks at $T \approx 65$ K and drops at higher T [34]. The measured thermal conductivity in YIG does exhibit a downward U-shaped behavior, but it is dominated by phonons. In Ref. [30] the change in the measured thermal conductivity of YIG with the application of a magnetic field was considered to be the full contribution of magnons. Actually, as can be seen in Fig. 3(b), the data correspond to the variation in the magnon contribution with the application of the field. The upper (blue) solid curve represents K_m calculated with Eq. (4) for $H = 0$ using the same exchange parameter as before and the relaxation rate in Eq. (5) with $c_{H3} = c_{H4} = 1.0$. The lower (red) curve was calculated with Eq. (4) for $H = 70$ kOe, with the contributions from 3- and 4-magnon relaxation in Eq. (5) multiplied by the factors with $c_{H3} = c_{H4} = 0.9$. These factors were determined by adjusting the theory to the experimental data of Ref. [30] shown in Fig. 3(b). They are close to the factors calculated in the magnon relaxation rate using the procedure of Refs. [15,39,40] for $H = 70$ kOe, $T = 10$ K. The reduction in the relaxation is attributed to the decrease in the number of thermal magnons involved in the scattering processes. Due to the decrease in the relaxation rate with field, for temperatures above 10 K, the conductivity K_m ($H = 70$ kOe) increases with temperature faster than K_m ($H = 0$), so that the difference between the two exhibits the peak observed experimentally [30].

The results described so far suggest a procedure to find reliable values for the thermal properties of magnons at room temperature, which are important to help in clarifying the origin of the spin Seebeck effect in YIG, a subject of current controversy [15,34,41–44]. As remarked in Ref. [34], the well-known expressions for the magnon specific heat C_m and thermal conductivity K_m valid for low temperatures completely fail at $T = 300$ K. The calculation of C_m and K_m at elevated temperatures using the appropriate magnon dispersion and relaxation rate and integration over a finite Brillouin zone leads to good estimates [34]. However, to obtain more reliable values one needs experimental data to determine some adjustable parameters in the calculation, such as the magnon zone-boundary frequency, the size of the Brillouin zone, and relaxation rates. Although the thermal properties are dominated by phonons and the absolute magnon contributions cannot be measured directly, the idea is to use the procedure of Refs. [28–30] of measuring the changes in the magnon contributions caused by the application of elevated magnetic fields. This should be done at the highest possible temperature so as to determine the adjustable parameters in the spin-wave calculation such that the results can be reliably extrapolated to room temperature.

Figure 4 shows the temperature variation of C_m and K_m calculated as in Ref. [34], using Eqs. (3) and (4), with the dispersion relation in Eq. (1) with $\omega_{ZB}/2\pi = 6$ THz and the

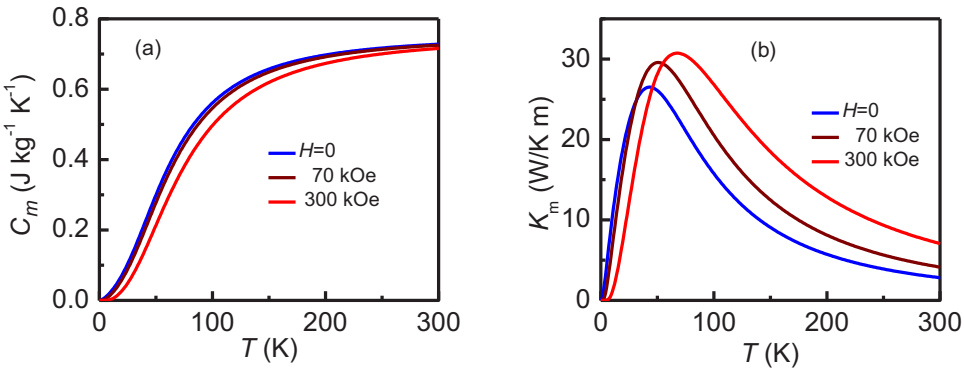

FIG. 4. (Color online) Temperature dependence of the magnon specific heat in (a) and magnon thermal conductivity in (b) at various values of the applied magnetic field H calculated with Eqs. (3) and (4) using the dispersion relation in Eq. (1) and the relaxation rate in Eq. (5).

relaxation rate in Eq. (5), with the appropriate factors for three values of the field, $H = 0$, 70, and 300 kOe. As can be seen in Fig. 4, the changes in C_m and K_m produced by $H = 70$ kOe relative to the zero-field values in the range $50 < T < 100$ K are quite small and would be in the noise level in the measurements of Ref. [30]. However, with a field of $H = 300$ kOe, which is available at some large facilities in several countries, the changes in C_m and K_m relative to the zero-field values are more significant and should be detectable. In particular, it is notable that in the range $50 < T < 100$ K, the magnon thermal conductivity increases with the application of a large field and represents several percent of the phonon contribution. As mentioned earlier, this fact results from the decrease in the magnon relaxation rate due to the smaller number of thermal magnon scatterers at higher fields. At 50 K the spin-wave damping is dominated by 3-magnon processes and at 100 K by 4-magnon. Thus, measurements of the temperature dependences of the change in K_m with $H = 0$ and 300 kOe in the range $50 < T < 100$ K should allow a good determination of the adjustable parameters in the spin-wave calculation to yield reliable values for C_m and K_m at room temperature.

IV. SUMMARY

In summary, we have used spin-wave theory to calculate the magnon specific heat and thermal conductivity in yttrium iron garnet under high magnetic fields. The calculations are compared with recent measurements of Boona and Heremans [30]. We have shown that in order to freeze out the magnon contribution to reduce the specific heat at $T = 10$ K to 10% of its zero-field value it is necessary to apply a field of 300 kOe. With the field of 70 kOe used in Ref. [30], C_m is reduced only to 2/3 of its zero-field value. The calculated changes in C_m and K_m agree very well with data. Based on the good agreement between theory and data we propose that by measuring the changes in the thermal properties in the range $50 < T < 100$ K, with $H = 0$ and $H = 300$ kOe, one could accurately determine the magnon thermal properties in YIG at room temperature, which should be helpful for testing models for the spin Seebeck effect in this material.

ACKNOWLEDGMENTS

This work was supported by Conselho Nacional de Desenvolvimento Científico e Tecnológico (CNPq), Coordenação de Aperfeiçoamento de Pessoal de Nível Superior (CAPES), Financiadora de Estudos e Projetos (FINEP), and Fundação de Amparo à Ciência e Tecnologia do Estado de Pernambuco (FACEPE).

[1] Y. Kajiwara, K. Harii, S. Takahashi, J. Ohe, K. Uchida, M. Mizuguchi, H. Umezawa, K. Kawai, K. Ando, K. Takanashi, S. Maekawa, and E. Saitoh, Nature (London) **464**, 262 (2010).
[2] C. W. Sandweg, Y. Kajiwara, K. Ando, E. Saitoh, and B. Hillebrands, Appl. Phys. Lett. **97**, 252504 (2010).
[3] K. Ando, T. Na, and E. Saitoh, Appl. Phys. Lett. **99**, 092510 (2011).
[4] L. H. Vilela-Leão, C. Salvador, A. Azevedo, and S. M. Rezende, Appl. Phys. Lett. **99**, 102505 (2011).
[5] A. Hoffmann, IEEE Trans. Magn. **49**, 5172 (2013).
[6] K. Uchida, J. Xiao, H. Adachi, J. Ohe, S. Takahashi, J. Ieda, T. Ota, Y. Kajiwara, H. Umezawa, H. Kawai, G. E. W. Bauer, S. Maekawa, and E. Saitoh, Nat. Mater. **9**, 894 (2010).
[7] K. Uchida, H. Adachi, T. Ota, H. Nakayama, S. Maekawa, and E. Saitoh, Appl. Phys. Lett. **97**, 172505 (2010).
[8] K. Uchida, T. Nonaka, T. Ota, H. Nakayama, and E. Saitoh, Appl. Phys. Lett. **97**, 262504 (2010).
[9] E. Padrón-Hernández, A. Azevedo, and S. M. Rezende, Phys. Rev. Lett. **107**, 197203 (2011); R. O. Cunha, E. Padrón-Hernández, A. Azevedo, and S. M. Rezende, Phys. Rev. B **87**, 184401 (2013).
[10] I. Zutic and H. Dery, Nat. Mater. **10**, 647 (2011).
[11] G. E. W. Bauer, E. Saitoh, and B. J. van Wees, Nat. Mater. **11**, 391 (2012).
[12] L. Lu, Y. Sun, M. Jantz, and M. Wu, Phys. Rev. Lett. **108**, 257202 (2012).

[13] H. Adachi, K. Uchida, E. Saitoh, and S. Maekawa, Rep. Prog. Phys. **76**, 036501 (2013).
[14] M. B. Jungfleisch, T. An, K. Ando, Y. Kajiwara, K. Uchida, B. I. Vasyuchka, A. V. Chumak, A. A. Serga, E. Saitoh, and B. Hillebrands, Appl. Phys. Lett. **102**, 062417 (2013).
[15] S. M. Rezende, R. L. Rodríguez-Suárez, R. O. Cunha, A. R. Rodrigues, F. L. A. Machado, G. A. Fonseca Guerra, J. C. López Ortiz, and A. Azevedo, Phy. Rev. B **89**, 014416 (2014).
[16] S. R. Boona, R. C. Myer, and J. P. Heremans, Energy Environ. Sci. **7**, 885 (2014).
[17] M. Sparks, *Ferromagnetic Relaxation* (Mc Graw-Hill, New York, 1964).
[18] R. M. White, *Quantum Theory of Magnetism*, 3rd ed. (Springer, Berlin, 2007).
[19] A. A. Serga, A. V. Chumak, and B. Hillebrands, J. Phys. D: Appl. Phys. **43**, 264002 (2010).
[20] S. M. Rezende and F. R. Morgenthaler, J. Appl. Phys. **40**, 524 (1969); **40**, 537 (1969).
[21] Y. K. Fetisov, P. Kabos, and C. E. Patton, IEEE Trans. Magn. **34**, 259 (1998).
[22] S. M. Rezende and F. M. de Aguiar, Proc. IEEE **78**, 893 (1990).
[23] B. A. Kalinikos, N. G. Kovshikov, and A. N. Slavin, Pis'ma Zh. Eksp. Teor. Fiz. **38**, 343 (1983) [JETP Lett. **38**, 413 (1983)].
[24] S. M. Rezende, F. M. de Aguiar, and O. F. de Alcantara Bonfim, J. Magn. Magn. Mater. **54–57**, 1127 (1986).
[25] S. O. Demokritov, V. E. Demidov, O. Dzyapko, G. A. Melkov, A. A. Serga, B. Hillebrands, and A. N. Slavin, Nature (London) **443**, 430 (2006).
[26] S. M. Rezende, Phys. Rev. B **79**, 174411 (2009).
[27] *Solid State Physics*, edited by M. Wu and A. Hoffmann (Academic, New York, 2013), Vol.64.
[28] R. L. Douglass, Phys. Rev. **129**, 1132 (1962).
[29] D. Walton, J. E. Rives, and Q. Khalid, Phys. Rev. B **8**, 1210 (1973).
[30] S. R. Boona and J. P. Heremans, Phys. Rev. B **90**, 064421 (2014).
[31] Y. Kohama, A. V. Sologubenko, N. R. Dilley, V. S. Zapf, M. Jaime, J. A. Mydosh, A. Paduan-Filho, K. A. Al-Hassanieh, P. Sengupta, S. Gangadharaiah, A. L. Chernyshev, and C. D. Batista, Phys. Rev. Lett. **106**, 037203 (2011).
[32] A. B. Harris, Phys. Rev. **132**, 2398 (1963).
[33] J. S. Plant, J. Phys. C: Solid State Phys. **16**, 7037 (1983).
[34] S. M. Rezende, R. L. Rodríguez-Suárez, J. C. Lopez Ortiz, and A. Azevedo, Phys. Rev. B **89**, 134406 (2014).
[35] C. Kittel, *Quantum Theory of Solids*, 2nd revised printing (Wiley, New York, 1987).
[36] W. B. Yelon and L. Berger, Phys. Rev. B **6**, 1974 (1972).
[37] A. N. Anisimov and A. G. Gurevich, Fiz. Tverd. Tela **18**, 38 (1976).
[38] B. Y. Pan, T. Y. Guan, X. C. Hong, S. Y. Zhou, X. Qiu, H. Zhang, and S. Y. Li, Europhys. Lett. **103**, 37005 (2013).
[39] S. M. Rezende and R. M. White, Phys. Rev. B **14**, 2939 (1976).
[40] S. M. Rezende and R. M. White, Phys. Rev. B **18**, 2346 (1978).
[41] J. Xiao, G. E. W. Bauer, K. C. Uchida, E. Saitoh, and S. Maekawa, Phys. Rev. B **81**, 214418 (2010).
[42] M. Schreier, A. Kamra, M. Weiler, J. Xiao, G. E. W. Bauer, R. Gross, and S. T. B. Goennenwein, Phys. Rev. B **88**, 094410 (2013).
[43] M. Agrawal, V. I. Vasyuchka, A. A. Serga, A. D. Karenowska, G. A. Melkov, and B. Hillebrands, Phys. Rev. Lett. **111**, 107204 (2013).
[44] S. Hoffman, K. Sato, and Y. Tserkovnyak, Phys. Rev. B **88**, 064408 (2013).